TEM investigation of the influence of dose rate on radiation damage and deuterium retention in tungsten

W.Chrominski[1]*, L. Ciupinski[1], P. Bazarnik[1], S. Markelj[2], T.Schwarz-Selinger[3]

[1]*Faculty of Materials Science and Engineering, Warsaw University of Technology, Woloska 141, 02-507 Warsaw, Poland*

[2]*Jožef Stefan Institute, Jamova cesta 39, 1000 Ljubljana, Slovenia*

[3]*Max-Planck-Institut für Plasmaphysik, Boltzmannstrasse 2, D-85748 Garching, Germany*

*e-mail: witold.chrominski@pw.edu.pl

Abstract

Tungsten targets were first irradiated with high energy W^{6+} ions (20MeV) with different dose rates at 800 K and then loaded with deuterium at room temperature to decorate the displacement damage created in the first step. Detailed microstructure investigations were performed and compared with calculated damage profiles and deuterium depth profiles to link defect characteristics with the ability to retain hydrogen isotopes. Results directly indicate that depending on the used dose rate dislocation density and characteristics change. However, deuterium retention does not. Thus, we conclude that overall dislocation density does not affect deuterium retention significantly. Changes in D retention were observed as function of the depth of the damaged zone. Variations of dislocation density were also depth dependent. Consequently, we link changes in D retention with the dislocation presence, number of implanted tungsten ions and other point defects. The latter seem to affects D retention the most.

Keywords: transmission electron microscopy, tungsten self-implantation, deuterium retention, ion radiation damage

1. Introduction

Tungsten is selected as one of the most prominent candidates for plasma facing components in future fusion devices. It combines satisfactory thermal stability with limited ability to store hydrogen isotopes. Fast neutrons generate a variety of defects in materials exposed to the severe fusion environment [1]. Since neutron sources are not widely available, those available do not offer the right energy spectrum, and samples treated this way exhibit radioactivity, other approaches to simulate displacement damage must be developed. One of them is to irradiate tungsten with high energy tungsten ions to induce defects similar to the ones produced by neutron bombardment [2,3]. The

mechanism of defects generation in such conditions can be studied by indirect techniques such as positron annihilation spectroscopy [4], which gives an insight into the type of generated defects. Some of the conclusions from these experiments were confirmed with microstructural TEM imaging like in-situ radiation experiments [5] or post-mortem observations performed on irradiated specimens [6].

Under real fusion conditions, multiple damage events may happen. They alter properties of pure tungsten. From this point of view, irradiation induced defects are particularly unwanted since hydrogen isotopes retention can significantly increase in damaged material [7]. Therefore, understanding the mechanisms responsible for hydrogen isotopes retention (mostly deuterium in laboratory conditions) is under investigation by various groups, for examples see [8–10]. Most of such studies focus on simulations or experimental determination of deuterium retention. Studies which combine microstructural observations with deuterium retention are lacking. Instead, conclusions are drawn from independent experiments. However, understanding of the underlying phenomena is hampered by the fact that a variety of irradiation procedures are utilized. This makes it often impossible to compare their results. In this study, we characterize the radiation damage with STEM and TEM on the very same samples were deuterium retention was studied previously, see [11]. Hence, this investigation links microstructure characteristics of samples irradiated with various dose rates with susceptibility of material to retain hydrogen isotopes.

2. Material and methods

Pure tungsten (99.97 weight %) was hot-rolled and recrystallized at 2000 K in vacuum for 2 minutes. Samples were subjected to self-implantation with 20MeV W^{6+} ions at 800 K to the level of 0.23dpa with three different average dose rates of 5.0×10^{-3}, 9.3×10^{-5}, 4.1×10^{-6} dpa/s. The time required to achieve the desired damage level varied depending on the rate used and equals 50, 3.36×10^{3} and 61.2×10^{3} s, respectively. For the two samples with the lower damage rate a focused W beam was scanned over the samples surface with scan frequencies of 1 kHz. For the fastest rate the focused beam was applied without scanning. The peak damage does rates are shown in Table 1.

Table 1 Damage rates in investigated samples

Average damage rate (dpa/s)	4.1×10^{-6}	9.3×10^{-5}	5.0×10^{-3}
Peak damage rate (dpa/s)	1.3×10^{-3}	5.8×10^{-3}	5.0×10^{-3}

The expected depth for the displacement damage is about 2 μm for this energy. After self-implantation samples were loaded with deuterium by a low-temperature deuterium plasma to decorate all the existing defects. A loading temperature of 295 K was chosen to minimize thermal de-trapping. No bias voltage was applied to the target to minimize the ion energy and hence avoid any additional damage

creation. A deuterium fluence of 1.5×10^{25} D/m^2 was chosen as to fill the whole damaged zone. For detailed description of the experiment see [11]. Concentration of implanted W ions as well as the primary displacements were calculated with the 'Quick Calculation of Damage' option of SRIM-2008.04 [12]. The primary damage was calculated by adding the "recoil" and "ion" displacements from the "vacancy.txt" output file and converting the sum with the ion fluence and the tungsten density to get a depth profile of the number of displaced target atoms and the damage dose in 'displacements per atom', in short 'dpa'. A displacement energy of 90 eV as recommended by the American Society for Testing and Materials [13] was used and a lattice binding energy of 0 eV.

Deuterium depth profiles were determined by the D(^{3}He,p)α nuclear reaction with eight different ^{3}He energies varying from 500 keV to 4.5 MeV to probe a sample depth of up to 7.4 μm. SIMNRA [14,15] and NRADC [16] was used for the deconvolution of all α and proton spectra measured at different ^{3}He ion energies.

Samples for TEM observations were cut with the use of a standard focused ion beam (Hitachi NB 5500) procedure and then milled gently by low energy Ar^+ plasma. General STEM observations were done with a Hitachi HD2700 operated at 200kV. TEM observations were performed with a JEOL JEM 1200EX II microscope with an acceleration voltage of 120kV. A double tilt holder was used for setting the desired diffraction conditions to assure comparability of results from different samples. Firstly, an observed grain was tilted to the closest [011] zone axis and then to <200> and <110> type two-beam conditions. The dislocation density was measured with use of the line intercept method, which has been already utilized in our previous works [6]. The image of each zone has been covered with the network of lines of known length (l). Then, number of intersections (n) between dislocation and experimental lines were counted. Dislocation density was calculated with the following formula:

$$\rho = \frac{n}{l\,t},$$

Where t is the specimen thickness estimated in focused ion beam system with use of electron column when lamella was positioned edge-on to the viewing direction. The error of the calculated dislocation density values are related mainly with uncertainties of thickness values estimated at 7%.

3. Results and discussion

3.1 Initial material

The material in the initial condition, before irradiation experiments, featured grain size of the order of tens of micrometers (Fig.1 (a)), which is typical for recrystallized tungsten. Grains interior are mostly free from dislocations, see Fig. 1 (b). STEM inspection has revealed some equilibrium dislocations,

nevertheless their amounts are too low to allow a meaningful calculation of the dislocation density results from STEM measurements. For this reason, we consider initial material as dislocation-free.

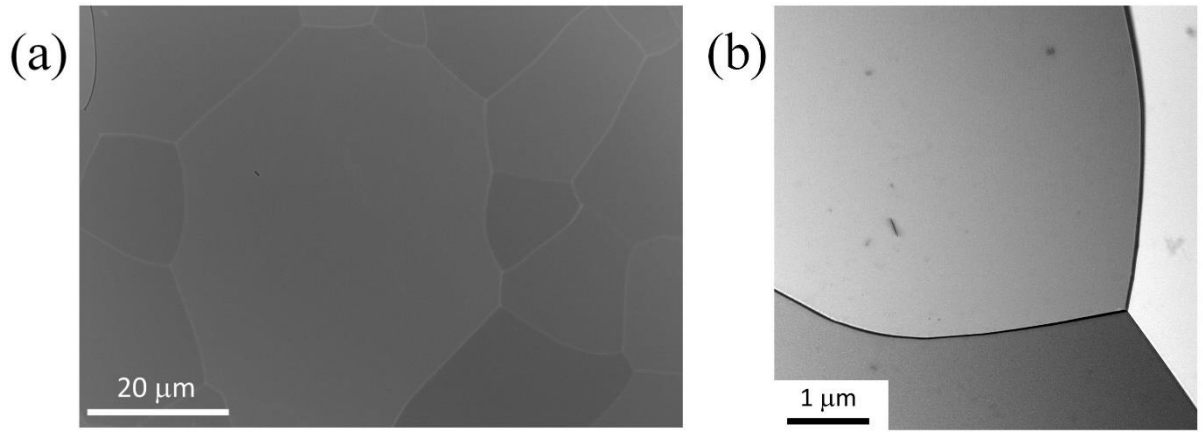

Fig. 1 Representative images of material in initial condition (a) SEM image of coarse grains (b) STEM image showing low density of dislocations in grain interiors.

3.2 Irradiation effects and deuterium retention

Fig. 2 shows images of dislocation structures within 1 μm from the surface of the target (located at the right side of the specimens, visible clearly in Fig. 2(b) and 2(c)). Differences in dislocations arrangements in samples treated with different damage dose rates can be seen. The sample with the lowest average dose rate (4.1×10^{-6} dpa/s), Fig.2(a), features short linear segments aligned predominantly with an angle of 60° relatively to themselves. The presence of homogenously distributed dots throughout the images is the result of FIB sample preparation, and should be treated as an artifact typically observed in such samples, especially with low dislocation densities [6,17]. The sample presented in Fig.2(b) experienced a higher average damage dose rate (9.3×10^{-5} dpa/s) as W ion implantation time was shortened to 3.36×10^{3} s. The dislocation appearance, similarly to the previous sample, is in the form of short straight-line segments inclined to each other. Additionally, some randomly distributed lines connect these regularly arranged ones. Moreover, the dislocation density is visibly higher in this specimen. The last specimen (Fig. 2 (c)) was damaged even more rapidly, since the irradiation process lasted only for 50 seconds, ending up with an average damage dose rate of 5.0×10^{-3} dpa/s. As a result, randomly distributed dislocation lines with no indication of any organized spatial arrangement are observed.

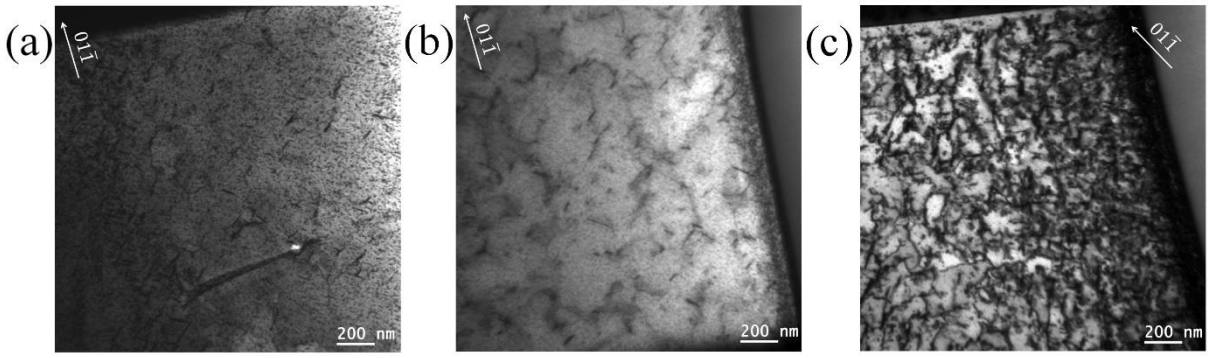

Fig. 2 TEM images of tungsten targets self-damaged with increasing average ion flux and hence damage rates (a) 4.1×10^{-6} dpa/s (b) 9.3×10^{-5} dpa/s (c) 5.0×10^{-3} dpa/s

Irradiation induced dislocation structures are being established with the atomic displacement caused by the interaction of the incident ion flux with the crystal lattice of the target. While the timescale for the primary damage is of the order of picoseconds it takes much longer time for atoms and ion-generated defects to rearrange themselves to create dislocations. It is postulated here that for this reason, rather slow damaging leads to the creation of more organized structures like the ones seen in Figs.2 (a) and (b). The former was irradiated with an average rate of 4.1×10^{-6} dpa/s and, in result organized dislocation segments were formed. When the average damaging rate was increased to 9.3×10^{-5} dpa/s (irradiation time shortened), an increased number of randomly distributed dislocation lines appeared due to more intense ion bombardment which inhibit complete arrangement of point defects to more organized structures. When irradiation was even more rapid (5.0×10^{-3} dpa/s) dislocation tangles were formed arbitrarily (Fig.2 (c)).

Fig.3 gathers three STEM images showing complete cross sections through the damaged zones of the samples prepared with the different damage dose rates. One can see that the depth affected by the 20 MeV W ion beam is the same in all specimens and agrees well with the SRIM calculation, see left graph in Fig.3. Three zones related with the differences in the amount of retained deuterium are placed at different distances from the surface of the specimens (top of the images). White lines in discussed microstructure images separate those zones in the images. Although less pronounced, the images show the same trend as observed with the TEM for the three different damage rates: the smallest and the medium damage rate samples show short straight-line segments of dislocations, the sample prepared with the highest damage rate shows more randomly distributed dislocation.

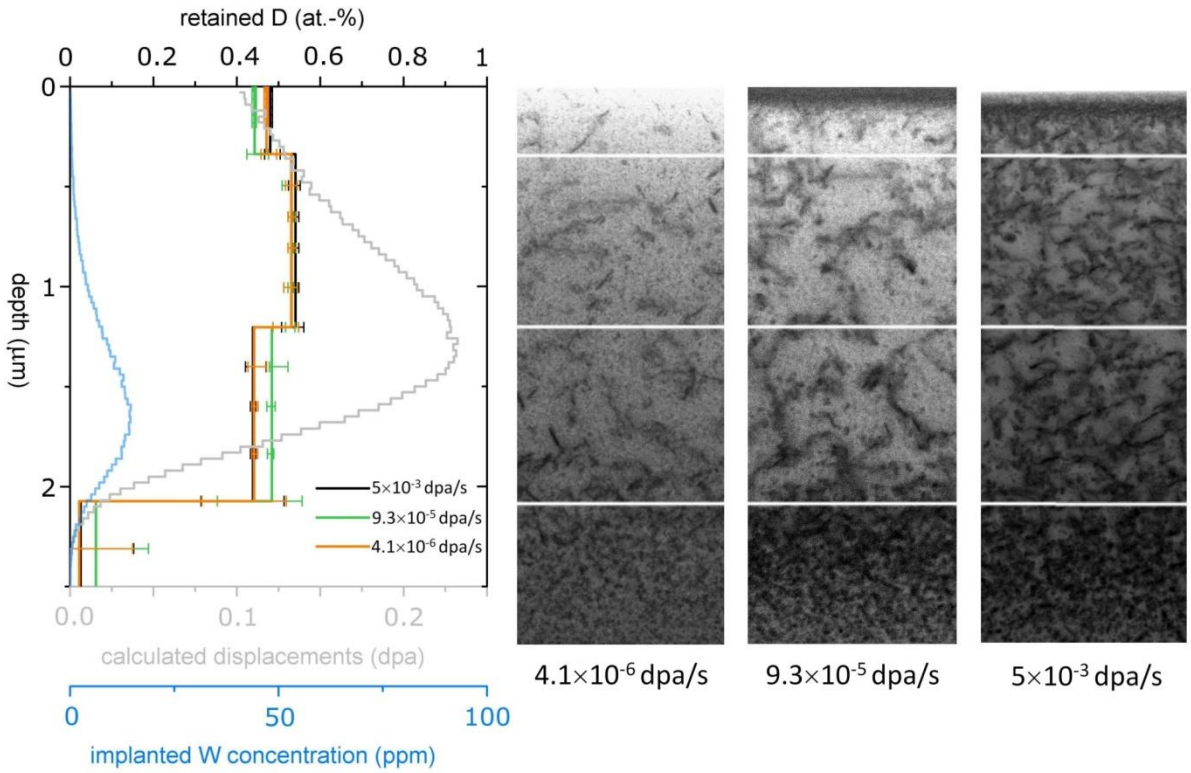

Fig. 3 Calculated primary displacement damage, concentration of implanted W, and measured deuterium concentration as function of depth together with a set of STEM images of tungsten targets damaged with different damage rates. The depth scale in the graph and the images are the same.

3.3 Dislocation structures

More detailed insight into dislocation structures from each zone is given in Figs. 4-6. The zone closest to the surface is affected by the W ions of the highest energy that enter the bulk and collide with crystalline lattice atoms. Concentration of implanted W ions (blue line in Fig. 3) is low in this zone as the incoming ions do not lose all their energy in this shallow layer of the material. Nevertheless, during collision they create Frenkel pairs. Due to the surface proximity many defects are believed to escape to the specimen surface and annihilate there. Since interstitials are more mobile than vacancies they are more subjected to this phenomena. As a result, the excess amount of vacancies remain within the lattice. Therefore, we assume that generated dislocations are the most likely vacancy-type in this zone because of the possibility of their rearrangement into other defects. This results in a relatively low level of observed displacement damage, even though, noticeable amounts of dislocations are still visible even in the sample damaged with the lowest rate, Fig. 4(a). Similarly to the observations from the general overview of the defected areas (Fig. 2) it can be seen that the character of dislocations appearance changes with the increasing damage rate and leads to formation of tangles for the highest rate, Fig. 4(c).

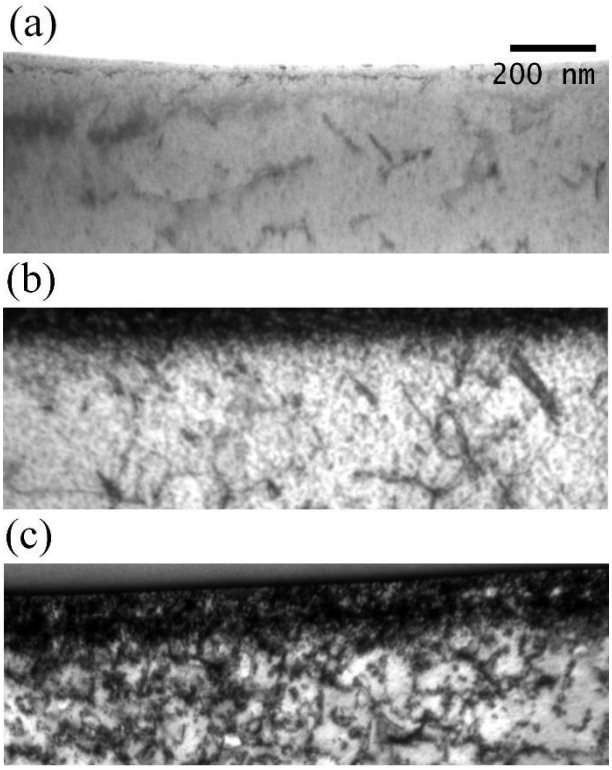

Fig. 4 TEM images of tungsten targets self-damaged with increasing average ion flux and hence damage rates – 0-300 nm zone (a) 4.1×10^{-6} dpa/s (b) 9.3×10^{-5} dpa/s (c) 5.0×10^{-3} dpa/s. Scale bar is the same for all images. Sample surface is on top.

In the middle (300-1100 nm) zone the most collisions events (primary ions, knock-out atoms as well as cascade atoms) take place. Graph in the Fig. 3 shows that displacement damage level increases here and reaches peak value closely to the area between this and the deepest one. Taking into account the classic cascade structure of vacancy-rich core surrounded by interstitials clusters, we assume that only a small fraction of implanted ions remain in this area. Multiple collisions with the lattice atoms led to formation of the mixture of self-interstitial dislocation loops together with the vacancy-type. According to modeling [18] and experimental [19] studies, the former are more likely to occur, but considerable amount of vacancy-type dislocations can be formed at 500ºC and higher temperature as well. Since mobile interstitials cannot escape through the surface in this zone they are subjected to create a dislocation loops. The appearance of dislocation structures is very similar to that present in the near-surface zone for all samples with the same dose rate. In the low and intermediate damage rate (Figs. 5 (a) and (b)) defects structures seem to be quite similar but more random dislocation lines were generated with the high dose rate, Fig. 5 (c).

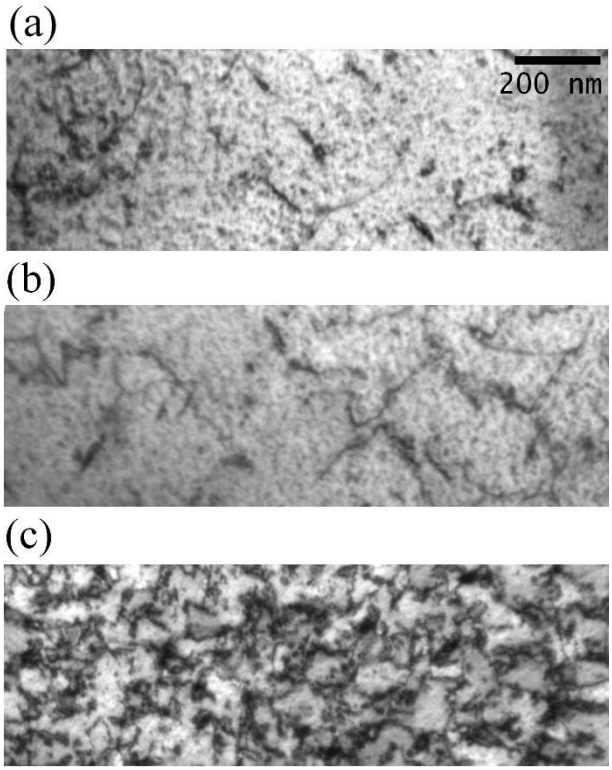

Fig. 5 TEM images of tungsten targets self-damaged with increasing average ion flux and hence damage rates – 300-1100 nm zone (a) 4.1×10^{-6} dpa/s (b) 9.3×10^{-5} dpa/s (c) 5.0×10^{-3} dpa/s. Scale bar is the same for all images

In the deepest zone there is a decreasing local level of displacement damage (see Fig. 3). In this area, incoming ions are losing their energy and remain in the lattice after the irradiation experiment. Decreasing displacement damage can be interpreted as lowered possibility to remove lattice atoms from their initial positions. For this two reasons, dislocations are the most likely formed by interstitials made by primary ions or atoms displaced from the zones above which were stopped in the deepest zone. Nevertheless, no special structures nor dislocation arrangements has been observed here. Images gathered in Fig. 6 collect observed structures in this zone. They remain similar the two previously discussed. Figs. 6 (a) and (b) show isolated dislocation lines without any characteristic arrangements, while Fig. 6 (c) is a spontaneous dislocation tangle which differs from those created by lower dose rates.

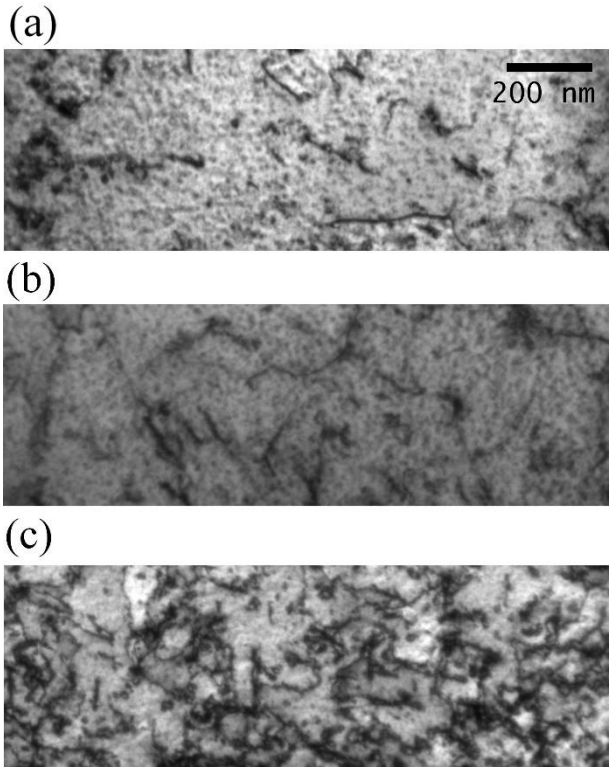

Fig. 6 TEM images of tungsten targets self-damaged with increasing average ion flux and hence damage rates – 1100-2100 nm zone (a) 4.1×10^{-6} dpa/s (b) 9.3×10^{-5} dpa/s (c) 5.0×10^{-3} dpa/s. Scale bar is the same for all images

3.4 Dislocations and deuterium retention

As a next step, dislocations densities have been calculated, see Table 2. A general trend can be seen for each sample. The dislocation density is slightly higher in the near-surface zone down to 300 nm, drops slightly down to 1100 nm and then raises again towards the end of range.

As can be noticed, in the three depth profiles in Fig.3, the D retention seems to be independent from the applied dose rate and dislocations arrangement generated during 20 MeV W irradiation. The depth profiles follow the same tendency for each sample. Slight increase in retained deuterium content observed in the zone between 300 and 1100 nm is present for all samples regardless of dislocation structures. Interestingly, the measured dislocation density and D retention exhibit opposite behavior – the middle zone features the lowest value of dislocation density and the highest D retention. Therefore, we can state that the morphology of the dislocations structure or apparent dislocation density does not affect deuterium retention even at these low exposure temperatures.

Table 2 Dislocation densities ($\times 10^{14}$ $1/m^2$) from the three zones located at different depths (characterized by different deuterium retention).

Average damage rate (dpa/s)		4.1×10^{-6}	9.3×10^{-5}	5.0×10^{-3}
Distance from the specimen`s surface	0-300 nm	0.75 ±0.061	0.83 ±0.066	1.50…±0.079
	300-1100 nm	0.66 ±0.035	0.78 ±0.075	1.44…±0.096
	1100-2100 nm	0.92 ±0.074	1.01 ±0.053	1.54 ±0.081

To support this statement an estimation of D atoms to be hold by a single dislocation was done. An approximate value of 0.5 at.% retention (see graph in Fig. 3) were obtained from TDS experiments in all zones. When multiplied by the tungsten density ($6.32 \times 10^{28} \frac{W\ at}{m^3}$) a number of D atoms in the volume unit can be calculated - $3.16 \times 10^{26} \frac{D\ at}{m^3}$. Number of dislocation lines can be obtained by dividing calculated values (Table 2) by the sample thickness (for simplification rounded values of density - $1 \times 10^{14} \frac{1}{m^2}$, and thickness $100nm = 10^{-7}m$ were used) gives $1\times 10^{21} \frac{1}{m^3}$. When D atoms density is divided by the dislocation volume density number of D atoms hold by a single dislocation line is estimated. In our experiments, this value is 316000 D atoms per dislocation. When compared to the values used in computer simulations done by other authors – up to 15 D atoms per dislocation [20–22] - it can be seen that our value is more than 20000 times higher. This result indicates that dislocations in our samples gives rather negligible effect on the retention and other, more effective mechanisms of D retention should be considered.

The only microstructural factor which links directly with changes in D retention is a slight drop of dislocation density in the middle (300-1100 nm) zone. However, as shown before this effect itself is rather meaningless in this terms. To find other microstructural reason of these results phenomena occurring under irradiation must be carefully evaluated. According to the studies of mechanism behind the formation of dislocation structures during irradiation and discussion from Section 3.3, the process can be split into stages including: 1) generation of point defects – vacancies and interstitials during collision between lattice atoms and incoming ions, 2) their rearrangement into agglomerates and 3) finally into new dislocations [5,6]. It means that the drop of dislocation density in the middle zone can be associated with increased amounts of point defects, particularly vacancies. As discussed in Section 3.3, due to limited ability of interstitials to annihilate on the surface, dislocations in this region are believed to be interstitial type mostly. Then, vacancies created during incoming ions collisions with the lattice are stored since they cannot interact with interstitials involved in dislocations. Thanks to this, an increased amount of vacancies are believed to be present in this region when compared to the other two zones.

At this stage of our studies it remains unclear, why vacancies supposedly in abundance in that zone do not rearrange into dislocations. However, it is known that diffusion of vacancies is rather limited in tungsten [23]. Formation of a vacancy loop requires a particular number of vacancies, above 30 according to [18]. Availability of more vacancies within the short distance of the diffusion range from an established dislocation loop, might be insufficient to "produce" new loops and thus, only vacancy clusters form. In the 1100-2100 nm zone, one can notice locally an increased dislocation density. Concurrently, this region features the highest concentration of implanted W ions (blue line in Fig. 3). As shown in [23], the fraction of interstitial loops is increased, relatively to vacancy-type, in regions of increased damage and excess of interstitials. In terms of D retention, it should be noted that vacancies and their clusters feature a higher deuterium detrapping energy of 1.45 and 1.85 eV, respectively compared to 0.85 eV reported for dislocations [24]. Then, no significant outgassing from dislocations is expected during desorption experiments. As shown in our rough estimation on dislocation effect on D atoms retention the dislocation density should be at least 20000 times higher to be able to store such an amount of hydrogen. Our investigations confirm that point defects and their agglomerates are of major importance when concerning deuterium trapping. Vacancies and clusters have been already shown to have significant effect on deuterium retention in tungsten targets [25].

4. Summary

In summary, our work shows that dislocation networks in tungsten samples prepared by self-implantation with different damage dose rate vary with the applied dose rate and depth of W ions penetration. We observed different dislocations density for the different damage dose, increasing with the damage dose. Slight differences in the dislocation types were observed in three damaging zones. Higher dislocation density in the deepest zone is related with rearrangement of interstitials which does not impact D storage. D retention drops here due to lowered vacancies concentration. The density of dislocations is five orders of magnitude lower than the density of the defects that trap deuterium for all damage rates and for this reason we conclude that the density of dislocation is too low to influence on D retention. We conclude that vacancies and vacancy clusters are the most important defects in terms of deuterium retention in tungsten.

Acknowledgements

This work has been carried out within the framework of the EUROfusion Consortium and has received funding from the EURATOM research and training programme 2014–2018 and 2019-2020 under grant agreement No 633053. The views and opinions expressed herein do not necessarily reflect those of the European Commission.

The Polish authors also acknowledge the financial support from the Polish Ministry of Science and Higher Education, grant no. 3987/H2020-Euratom/2018/2.

W. Chrominski is supported by the Foundation for Polish Science (FNP) within the START programme.

Data availability

The raw data required to reproduce these findings cannot be shared at this time as the data also forms part of an ongoing study

References

[1] V. Barabash, G. Federici, M. Rödig, L.L. Snead, C.H. Wu, Neutron irradiation effects on plasma facing materials, J. Nucl. Mater. 283–287 (2000) 138–146. doi:10.1016/S0022-3115(00)00203-8.

[2] G.S. Was, Fundamentals of Radiation Materials Science, 2007. doi:10.1007/978-3-540-49472-0.

[3] O. V. Ogorodnikova, V. Gann, Simulation of neutron-induced damage in tungsten by irradiation with energetic self-ions, J. Nucl. Mater. 460 (2015) 60–71. doi:10.1016/j.jnucmat.2015.02.004.

[4] I. Uytdenhouwen, T. Schwarz-Selinger, J.W. Coenen, M. Wirtz, Mechanical and Microstructural Changes in W Due to Irradiation Damage, Phys. Scr. T167 (2016).

[5] X. Yi, M.L. Jenkins, M.A. Kirk, Z. Zhou, S.G. Roberts, In-situ TEM studies of 150 keV W+ion irradiated W and W-alloys: Damage production and microstructural evolution, Acta Mater. 112 (2016) 105–120. doi:10.1016/j.actamat.2016.03.051.

[6] J. Grzonka, Ciupiński, J. Smalc-Koziorowska, O. V. Ogorodnikova, M. Mayer, K.J. Kurzydłowski, Electron microscopy observations of radiation damage in irradiated and annealed tungsten, Nucl. Instruments Methods Phys. Res. Sect. B Beam Interact. with Mater. Atoms. 340 (2014) 27–33. doi:10.1016/j.nimb.2014.07.043.

[7] B. Tyburska, V.K. Alimov, O. V. Ogorodnikova, K. Schmid, K. Ertl, Deuterium retention in self-damaged tungsten, J. Nucl. Mater. 395 (2009) 150–155. doi:10.1016/j.jnucmat.2009.10.046.

[8] K. Schmid, J. Bauer, T. Schwarz-Selinger, S. Markelj, U. V. Toussaint, A. Manhard, et al., Recent progress in the understanding of H transport and trapping in W, Phys. Scr. (2017) 77494999. doi:10.1088/1402-4896/aa8de0.

[9] A. Založnik, S. Markelj, T. Schwarz-Selinger, K. Schmid, Deuterium atom loading of self-damaged tungsten at different sample temperatures, J. Nucl. Mater. 496 (2017) 1–8. doi:10.1016/j.jnucmat.2017.09.003.

[10] M.J. Simmonds, Y.Q. Wang, J.L. Barton, M.J. Baldwin, J.H. Yu, R.P. Doerner, et al., Reduced deuterium retention in simultaneously damaged and annealed tungsten, J. Nucl. Mater. 494 (2017) 67–71. doi:10.1016/j.jnucmat.2017.06.010.

[11] T. Schwarz-Selinger, Deuterium retention in MeV self-implanted tungsten: Influence of

damaging dose rate, Nucl. Mater. Energy. 12 (2017) 683–688. doi:10.1016/j.nme.2017.02.003.

[12] www.srim.org, (n.d.).

[13] ASTM E521-96 Standard Practice for Neutron Radiation Damage Simulation by Charge-Particle Irradiation, Annual Book of ASTM Standards vol 12.02, n.d.

[14] M. Mayer, SIMNRA User's Guide, Report IPP 9/113, Max-Planck-Instutut für Plasmaphysik, Garching, 1997.

[15] http://www.rzg.mpg.de/~mam, (n.d.).

[16] K. Schmid, U. Von Toussaint, Statistically sound evaluation of trace element depth profiles by ion beam analysis, Nucl. Instruments Methods Phys. Res. Sect. B Beam Interact. with Mater. Atoms. 281 (2012) 64–71. doi:10.1016/j.nimb.2012.03.024.

[17] Ciupiński, O. V. Ogorodnikova, T. Płociński, M. Andrzejczuk, M. Rasiński, M. Mayer, et al., TEM observations of radiation damage in tungsten irradiated by 20 MeV W ions, Nucl. Instruments Methods Phys. Res. Sect. B Beam Interact. with Mater. Atoms. 317 (2013) 159–164. doi:10.1016/j.nimb.2013.03.022.

[18] A.E. Sand, S.L. Dudarev, K. Nordlund, High-energy collision cascades in tungsten: Dislocation loops structure and clustering scaling laws, Epl. 103 (2013). doi:10.1209/0295-5075/103/46003.

[19] X. Yi, M.L. Jenkins, K. Hattar, P.D. Edmondson, S.G. Roberts, Characterisation of radiation damage in W and W-based alloys from 2 MeV, Acta Mater. 92 (2015) 163–177. doi:10.1016/j.actamat.2015.04.015.

[20] P. Grigorev, A. Bakaev, D. Terentyev, G. Van Oost, J. Noterdaeme, E.E. Zhurkin, Interaction of hydrogen and helium with nanometric dislocation loops in tungsten assessed by atomistic calculations, Nucl. Inst. Methods Phys. Res. B. 393 (2017) 164–168. doi:10.1016/j.nimb.2016.10.036.

[21] V. Dubinko, P. Grigorev, A. Bakaev, D. Terentyev, G. Van Oost, F. Gao, et al., Dislocation mechanism of deuterium retention in tungsten under plasma implantation, J. Phys. Condes. Matter. 26 (2014) 395001. doi:10.1088/0953-8984/26/39/395001.

[22] A. Bakaev, P. Grigorev, D. Terentyev, A. Bakaeva, E.E. Zhurkin, Trapping of hydrogen and helium at dislocations in tungsten : an ab initio study, Nucl. Fusion. 57 (2017) 126040.

[23] X. Yi, M.L. Jenkins, M. Briceno, S.G. Roberts, Z. Zhou, M.A. Kirk, In situ study of self-ion irradiation damage in W and W-5Re at 500°C, Philos. Mag. 93 (2013) 1715–1738. doi:10.1080/14786435.2012.754110.

[24] O. V. Ogorodnikova, B. Tyburska, V.K. Alimov, K. Ertl, The influence of radiation damage on the plasma-induced deuterium retention in self-implanted tungsten, J. Nucl. Mater. 415 (2011) S661–S666. doi:10.1016/j.jnucmat.2010.12.012.

[25] Y. Jin, K.B. Roh, M.H. Sheen, N.K. Kim, J. Song, Y.W. Kim, et al., Enhancement of deuterium retention in damaged tungsten by plasma-induced defect clustering, Nucl. Fusion. 57 (2017). doi:10.1088/1741-4326/aa856c.